

Susan C. van den Heever\*, Gustavo G. Carrió, William R. Cotton and William C. Straka  
 Department of Atmospheric Science, Colorado State University, Fort Collins, Colorado

## 1. INTRODUCTION

Dust serves as effective cloud condensation nuclei (CCN), giant CCN (GCCN) and ice forming nuclei (IFN). Dust can therefore have significant effects on the nucleation of ice and liquid water, which in turn may affect other microphysical and dynamical characteristics of convective storm systems. It has been estimated that 60% of dust can be traced to human activities. Unusually high aerosol concentrations were observed on 28 and 29 July during the CRYSTAL-FACE (Cirrus Regional Study of Tropical Anvils and Cirrus Layers – Florida Area Cirrus Experiment) field program conducted by the National Aeronautics and Space Administration (NASA) over the Florida peninsula during July 2002 (Jensen et al., 2004). These have been attributed to the penetration of Saharan dust over the peninsula during this time (DeMott et al., 2003; Sassen et al., 2003). The goal of the research presented here is thus to investigate the impacts that increasing the concentrations of IFN, CCN and GCCN may have on the characteristics of the convective and anvil stages of Florida convection, through the use of a cloud-resolving numerical model.

## 2. METHODS

### 2.1 Mesoscale Model

The Regional Atmospheric Modeling System developed at Colorado State University (RAMS@CSU) was chosen to achieve the goal stated above (Pielke et al., 1992; Cotton et al., 2003). Four nested grids were employed, the horizontal grid spacings of which were 40, 10, 2 and 0.5 km for grids 1 to 4, respectively. The location of these grids is shown in Figure 1. The fourth grid was moved in order to follow the developing anvils. A stretched 36-level grid was used in the vertical. RAMS was initialized at 12Z with 40km ETA data, and the simulations were performed for 12 hours.

\* *Corresponding author address:* Susan C. van den Heever, Department of Atmospheric Science, Colorado State University, Fort Collins, CO 80526; email: sue@atmos.colostate.edu.

All the microphysical species (cloud water, rain, pristine ice, snow, aggregates, graupel and hail) in RAMS were activated, and both hydrometeor mixing ratios and number concentrations were predicted through the use of the two-moment bulk microphysics scheme (Meyers et al., 1997). CCN, GCCN and IFN concentrations are all considered prognostic variables in RAMS (Saleeby and Cotton, 2004).

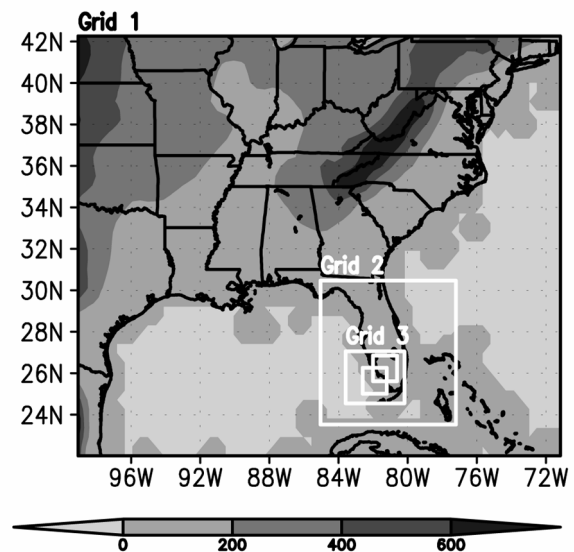


Figure 1: The topography (m) and location of grids 1 through 4 used in the simulations described in the text. Both locations of grid 4 are shown.

### 2.2 Data and Experiment Design

During the CRYSTAL-FACE field campaign, IFN were measured using a continuous flow diffusion chamber (Rogers et al., 2001) on board the Citation aircraft. The measurements were made at  $-36^{\circ}\text{C}$  and  $\sim 86\%$  RH with respect to water ( $123\%$  RH with respect to ice). A continuous flow CCN instrument on the Twin Otter was used to measure CCN (VanReken et al., 2003). Measurements were made at 0.7% supersaturation. GCCN were determined using the Droplet Measurement Technologies' cloud and aerosol spectrometer on board the WB-57 aircraft (<http://www.dropletmeasurement.com>). The

spectrometer is capable of measuring sizes from 0.3 to 50  $\mu\text{m}$ .

Generalized vertical profiles of CCN, GCCN and IFN concentrations were obtained for a “dusty” (OBS) (28 July) and “clean” day (CLN) (18 July) (Figure 2). These profiles, which were based on measurements made by Paul DeMott of the Colorado State University Simulation Laboratory, were used to initialize the aerosol fields of the model. Eight different sensitivity tests were then performed in which the initial aerosol concentrations were varied independently and simultaneously as shown in Table 1. A factor separation analysis (Stein and Alpert, 1993) was also conducted to determine which aerosol species has the predominant effect on various cloud and properties and the surface precipitation.

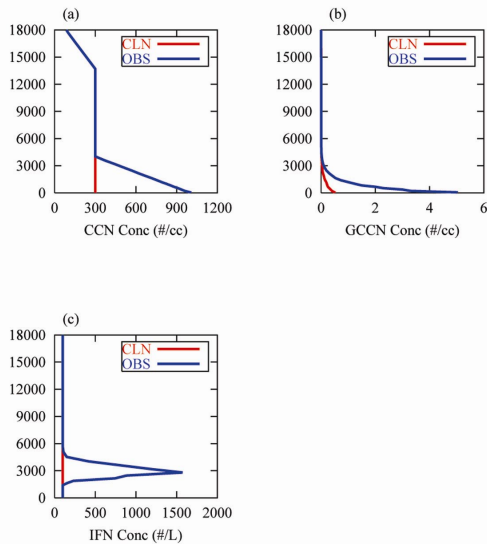


Figure 2: Generalized clean (CLN) and observed (OBS) vertical profiles of (a) CCN, (b) GCCN and (c) IFN concentrations used to initialize the sensitivity tests described in the text.

### 3. RESULTS

#### 3.1 Storm System Development

Vertically-integrated condensate for the CLN and OBS cases, as well as the corresponding satellite imagery, is shown in Figure 3. In both cases convection develops to the southwest of Lake Okeechobee and tracks toward the west and

Table 1: Aerosol characteristics of the conducted sensitivity tests

Name	CCN	GCCN	IFN
CLN	Clean	Clean	Clean
Exp2	Observed	Clean	Clean
Exp3	Clean	Observed	Clean
Exp4	Clean	Clean	Observed
Exp5	Observed	Observed	Clean
Exp6	Observed	Clean	Observed
Exp7	Clean	Observed	Observed
OBS	Observed	Observed	Observed

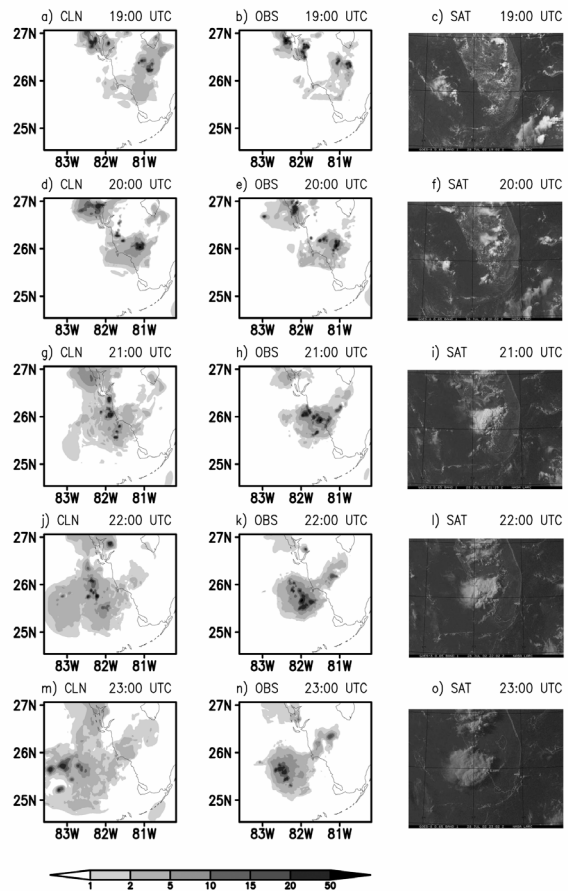


Figure 3: Vertically integrated condensate (shading, mm) for the CLN (a,d,g,j,m) and OBS (b,e,h,k,n) simulations and the corresponding visible satellite imagery (c,f,i,l,o) (figures used with the permission of Louis Nguyen, NASA Langley Research Center).

southwest, as is evident in the satellite imagery. Extensive anvil cirrus clouds develop in both simulations. Comparing the CLN and OBS simulations it is apparent that the anvil in the OBS case covers a smaller area but achieves greater maximum condensate amounts and is better organized than in the CLN case. The OBS is also a better representation of the actual observations. Increasing the aerosol concentrations therefore decreases the spatial area of the anvil, but increases the amount of water mass in a vertical column, both of which will impact the radiative forcing of the anvil.

The convection in both simulations tends to move offshore more rapidly than was observed. This appears to be due to stronger cold pools in the simulations that overwhelm the sea-breeze circulation more rapidly, thus allowing the convective cells to move off the coast earlier than in the observations. It should also be noted that the convection in the region of Fort Meyers (~26.5N, 82W) is not well-represented as this is beyond the northern grid boundary of grid 4.

### **3.2 Updraft Structure**

The location of updraft development, the number of convective cores that develop, the strength of these cores and the longevity of the updrafts differ significantly between the two simulations (not shown). The updrafts are wider, stronger and in closer proximity in the OBS case compared with those in the CLN case simulation. Density distributions of the vertical velocity at ~3200 m and ~7800m AGL demonstrates that updrafts occur throughout more of the domain and are stronger throughout the OBS case (Figure 4). The maximum updraft velocities are also achieved in the OBS case. The vertical velocities, averaged over the convective cores (defined as the grid points where the vertical velocity averaged between 5700m and 14700 m AGL is greater than or equal to  $1 \text{ m}\cdot\text{s}^{-1}$ ) also demonstrate these characteristics.

Examining the differences between the temporally-averaged (1800-0000 UTC) vertical velocities of the sensitivity tests and the CLN simulation between 8 and 10 km AGL shows that increasing all three nucleating aerosol types enhances the maximum updraft strengths throughout the troposphere through latent heat

release effects (not shown). However, increasing GCCN concentrations exclusively has the greatest effect on updraft strengths between 8 and 10 km AGL, followed by those of IFN. The impacts of increasing CCN alone is less than all the other sensitivity tests with the exception of the I+G case.

These vertical velocity results demonstrate several important points. Simply increasing aerosol concentrations can have a 3 to  $4 \text{ m}\cdot\text{s}^{-1}$  increase on the horizontally-averaged updraft strength, a significant effect given that these are horizontal averages, and not maximum quantities. Variations in aerosol concentrations therefore not only affect microphysical properties, but also have the potential to change the dynamics of the entire storm system. Previous research has focused primarily on how increases in CCN number concentrations tend to reduce warm rain efficiencies and increase cloud water contents (e.g. Warner and Twomey 1967; Albrecht 1989; Kaufman and Nakajima 1993; Borys et al. 1998; Rosenfeld 1999, 2000; Andreae et al. 2004). Greater amounts of liquid water is thus available to be transported vertically, which provides greater amounts of supercooled water that can freeze, the release of greater amounts of latent heat, and subsequent increases in updraft strength. While this is found in these simulations, the sensitivity tests indicate that enhanced GCCN and IFN concentrations have a greater impact on updraft strength during the mature and dissipating stages of convection, and that the effects of enhanced CCN concentrations are only dominant during the initial stages of convective development.

### **3.3 Microphysical Impacts**

Vertical profiles of the horizontally- and temporally-averaged liquid water and ice species within the updraft, represented as a difference between the sensitivity test and the CLN case, are shown in Figure 5. Between 2 and 5 km AGL, enhancement of all three aerosol species generally results in greater amounts of cloud water compared with the CLN case (Figure 5a). The sole enhancement of GCCN produces the most cloud water, followed by increases in both the CCN and GCCN concentrations. The contribution to cloud water in the IFN case occurs through the melting of the ice species such as ice crystals and aggregates. The melting level is at ~5 km AGL.

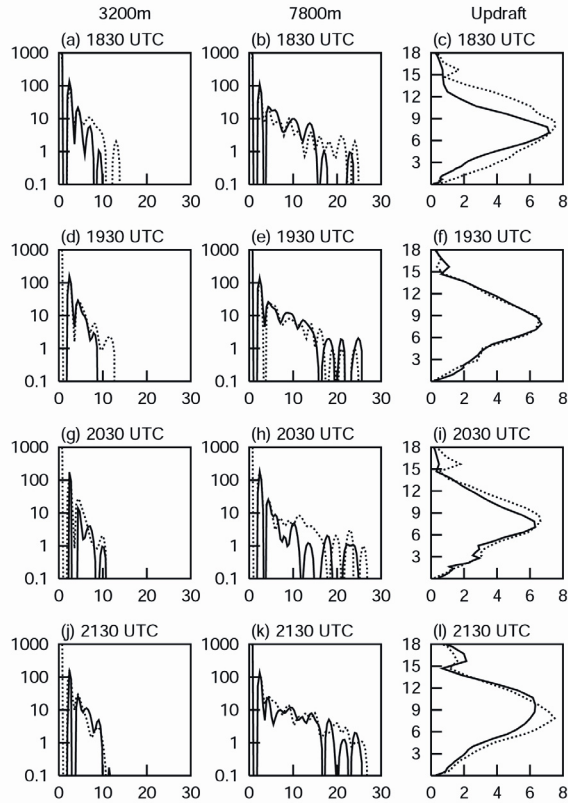


Figure 4: Density distribution of vertical velocity at ~3200m AGL (left column) and ~7800m AGL (middle column), and the horizontally averaged velocities within the updraft (right column) for the CLN (solid lines) and OBS (dotted lines) cases at hourly intervals starting at 1830 UTC. Abscissa is vertical velocity, and ordinate is number (on a log scale) for the density distributions and height (km) for the averaged velocities.

Between approximately 2 and 4 km AGL the CLN case is the most efficient warm rain producer, followed by the GCCN simulation in which the droplet distribution is wider, and the IFN case in which melting ice species contribute to rain (Figure 5b). The CCN sensitivity test is one of the least efficient rain producers, which supports previous findings regarding the impacts of CCN on warm rain production (e.g. Warner and Twomey, 1967; Albrecht 1989; Kaufman and Nakajima 1993; Borys et al. 1998; Rosenfeld 1999, 2000; Andreae et al. 2004). The test in which both CCN and GCCN are enhanced also reduces rainfall when compared with the CLN case. This is somewhat surprising in that a wider size distribution could be

expected to produce rainfall more efficiently. However the GCCN are depleted relatively quickly, thus reducing the ratio of GCCN to CCN. From the surface to 2 km AGL, increasing the GCCN and IFN concentrations enhances rain formation, whereas enhanced CCN concentrations have the greatest negative impact on surface rainfall.

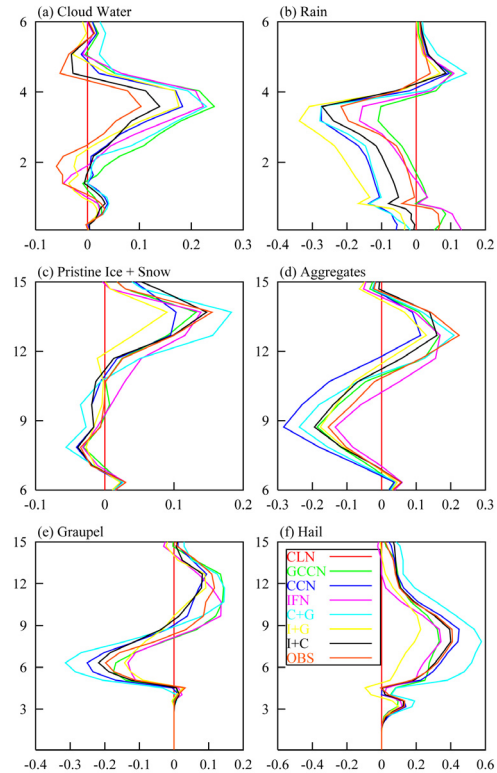


Figure 5: Vertical profiles of the difference between the sensitivity tests and the CLN simulation (red) for the horizontally- and temporally (1800-0000 UTC)-averaged (a) cloud water, (b) rain, (c) pristine ice + snow, (d) aggregates, (e) graupel and (f) hail mixing ratios within the updrafts. The profiles of the sensitivity tests are labeled in the key in (f). The abscissa is mixing ratio ( $\text{g.kg}^{-1}$ ) and the ordinate is height (km).

Between ~9.5 and 11 km AGL, increases in IFN concentrations lead to the same amount of ice crystals as produced by the rest of the sensitivity tests higher up, supporting previous observations that the presence of Saharan dust allows for ice nucleation at warmer temperatures (Schaefer, 1949; 1954; Isono et al, 1959; DeMott et al. 2003; Sassen et al. 2003). The anvil is also deeper in this case. Higher up, however, the C+G case

produces the greatest differences from the CLN case. This case produces large amounts of cloud water but relatively little rain, which means that relatively high LWCs are available for ice formation. Also, in the IFN case, which also produces high cloud water contents, the formation of ice at warmer temperatures deprives the upper levels of available moisture. All of the sensitivity tests produce greater amounts of ice compared with the CLN case due to the greater amounts of liquid water available.

Below ~9 km AGL, all the sensitivity tests result in a reduction in graupel compared with the CLN case, with those involving increased CCN concentrations having the greatest effect (Figure 5e). As the melting level (~ 5 km AGL) is approached, the differences between the simulations become insignificant. The trends in the hail mixing ratio differences below 9 km AGL are almost a mirror image of those of graupel, with most hail being produced in the C+G case. In this case, large amounts of cloud water are produced which will enhance riming of graupel, and force these hydrometeors into the hail category in which the hydrometeors are larger and may contain a greater percentage of liquid water on their surface. Because hail is also formed by the freezing of raindrops, and rain mixing ratios are greatest in the C+G case between 4 and 6 km AGL, they provide a major source for hail formation in this region.

The differences in vertical velocity and cloud water due to variations in aerosol concentrations suggest a possible microphysical-dynamical feedback mechanism. It was seen above that the enhanced GCCN case produces higher time-averaged cloud water mixing ratios than the enhanced CCN case. Examining the cloud water field at specific times demonstrates that during the initial stages of the storm, the enhanced CCN case produces more cloud water than the enhanced GCCN run, but this trend reverses during the mature and dissipating stages. A similar reversal was also seen for the vertical velocity field in that updrafts were stronger in the enhanced CCN case initially, but during the mature and dissipating stages the updrafts were stronger in the enhanced GCCN case. The following hypothesis is put forward: initially greater amounts of cloud water are produced in the enhanced CCN test, the contributions of which come primarily from the first cloud mode (the mode associated with CCN). The

associated release of latent heat produces the stronger updrafts. However, as the simulations progress and cloud water is transported vertically, the second mode of cloud water associated with GCCN becomes more important as this mode is more effective in ice phase interactions e.g. larger droplets are more effectively collected by ice particles, larger droplets undergo homogeneous freezing more rapidly. In the GCCN case, greater amounts of the second cloud water mode are produced, and hence the associated release of latent heat upon interacting with ice is greater. This results in the stronger updrafts in the GCCN case during the mature and dissipating stages. Stronger updrafts (in all cases) result in the more rapid production of cloud water and pristine ice, which in turn enhance the updraft strengths, and so the feedback cycle continues.

### **3.4 Accumulated Surface Precipitation**

Another aspect associated with convective storms that is affected by variations in aerosol concentrations is the accumulated surface precipitation. The accumulated surface precipitation for the sensitivity tests are shown in Table 2. It is apparent that by 1800 UTC, most surface precipitation has occurred in the IFN and GCCN cases, followed by the I+G case, all three of which produce more surface precipitation than the CLN case. All the sensitivity tests in which CCN were enhanced result in a decrease in the surface precipitation at this time. The dominance of the sensitivity tests in which IFN and GCCN concentrations are enhanced suggest a response similar to "dynamic seeding" concepts in which enhanced glaciation of convective clouds leads to dynamical invigoration of the clouds, larger amounts of processed water, and thereby enhanced rainfall at the ground (Simpson et al, 1967; Rosenfeld and Woodley, 1989; 1993). By 0000 UTC the total surface precipitation is greatest in the CLN case, demonstrating the reduction in surface precipitation associated with the increases in aerosol concentrations. Of the dust cases, increases in GCCN concentrations results in the most surface precipitation, followed by the enhancements of IFN. All the simulations involving CCN produce the least surface precipitation, even less than the observed case.

Table 2: Accumulated surface precipitation (acre-feet) for the 8 sensitivity tests described in the text, in descending order at 1800 and 0000 UTC.

1800 UTC		0000 UTC	
Exp Name	Magnitude (a-f)	Exp Name	Magnitude (a-f)
IFN	66608	CLN	442168
GCCN	65874	GCCN	368053
I+G	63487	I+G	352112
CLN	63289	IFN	349373
CCN	61741	OBS	346309
C+G	58275	CCN	344338
I+C	57700	I+C	330610
OBS	57008	C+G	327560

It is somewhat surprising that the CLN case produces more surface precipitation compared with the GCCN sensitivity test, given that the introduction of GCCN tend to widen the droplet spectrum and enhance warm rain processes. This may in part be attributed to the rapid depletion of GCCN through several different processes. The initial updraft development to the south of Lake Okeechobee occurs in regions that are rich in GCCN in the lower levels compared with that in the CLN case. Two hours later though, the updrafts in the CLN and GCCN cases are located within environmental air that have similar GCCN concentrations. In the GCCN case, GCCN concentrations are relatively low over the ocean where high relative humidities result in the formation of low-level clouds, and over land in association with the sea-breeze frontal passage which provides sufficient lift to nucleate droplets in the second cloud water, both of which deplete GCCN.

### 3.5 Precipitation Efficiency

The precipitation and anvil efficiencies for two 'dusty' (28 and 29 July 2002) and one relatively 'clean' (16 July 2002) day during the CRYSTAL-FACE field campaign have been calculated using radar data. The results of these calculations are shown in Table 3. It is apparent from these results that both the precipitation and anvil efficiencies increase with increasing concentrations in Saharan dust. Modeling studies of 16 and 29 July are

currently underway in order to compare the simulated precipitation and anvil efficiencies for all three days with those observed.

Table 3: Precipitation and Anvil Efficiencies for 16, 28 and 29 July 2003

DATE	Average Precipitation Efficiency	Average Anvil Efficiency
16 July 2002	24%	1%
28 July 2002	80%	5%
29 July 2002	59%	5%

## 4. CONCLUSIONS

The results presented above demonstrate that Saharan dust has a significant impact, not only on the microphysical characteristics of convective storms over Florida, but also on the dynamics, accumulated precipitation and precipitation efficiencies of such storms. These results also highlight that while the focus traditionally has been primarily on the influences of CCN, that the impacts of GCCN and IFN are of equivalent importance and need to be taken into account. Modeling studies of 16 and 29 July 2002 are currently underway. The results from these simulations will be compared with the findings from 28 July 2002.

## 5. ACKNOWLEDGEMENTS

Paul DeMott and Anthony Prenni of the Colorado State University Simulation Laboratory are acknowledged for providing us with the clean and observed aerosol profiles from the CRYSTAL-FACE field campaign. This research was funded by NASA under contract NAG5-11507.

## 6. REFERENCES

- Albrecht, B., 1989: Aerosols, cloud microphysics, and fractional cloudiness. *Science*, **245**, 1227-1230.
- Andreae, M.O., D. Rosenfeld, P. Artaxo, A.A. Costa, G.P. Frank, K.M. Longo, and M.A.F. Silva-Dias, 2004: Smoking rain clouds over the Amazon. *Science*, **303**, 1337-1342.

- Borys, R.D., D.H. Lowenthal, M.A. Wetzel, F. Herrera, A. Gonzalez, and J. Harris, 1998: Chemical and microphysical properties of marine stratiform cloud in the North Atlantic. *J. Geophys. Res.*, **103**, 22,073-22,085.
- Cotton, W.R., R.A. Pielke Sr., R.L. Walko, G.E. Liston, C.J. Tremback, H. Jiang, R.L. McAnelly, J.Y. Harrington, M.E. Nicholls, G.G. Carrio, and J.P. McFadden, 2003: RAMS 2001: Current status and future directions. *Meteor. Atmos. Phys.*, **82**, 5-29.
- DeMott, P.J., K. Sassen, M.R. Poellet, D. Baumgardner, D.C. Rogers, S. Brooks, A.J. Prenni, and S. M. Kreidenweis, 2003: African dust aerosols as atmospheric ice nuclei. *Geophys. Res. Lett.*, **30**, 10.1029/2003GL017410.
- Isono, K., M. Komabayasi, and A. Ono, 1959: The nature and origin of ice nuclei in the atmosphere. *J. Meteorol. Soc. Japan*, **37**, 211-233.
- Jensen, E., D. Starr, and O.B. Toon, 2004: Mission investigates tropical cirrus clouds. *EOS*, **85**, 45-50.
- Kaufman, Y.J., and T. Nakajima, 1993: Effect of Amazon smoke on cloud microphysics and albedo-analysis from satellite imagery. *J. Appl. Meteor.*, **32**, 729-744.
- Meyers, M.P., R.L. Walko, J.Y. Harrington, and W.R. Cotton., 1997: New RAMS cloud microphysics parameterization. Part II: The two-moment scheme. *Atmos. Res.*, **45**, 3-39.
- Pielke, R.A., W.R. Cotton, R.L. Walko, C.J. Tremback, W.A. Lyons, L.D. Grasso, M.E. Nicholls, M.D. Moran, D.A. Wesley, T.J. Lee, and J.H. Copeland, 1992: A comprehensive meteorological modeling system – RAMS. *Meteor. Atmos. Phys.*, **49**, 69-91.
- Rogers, D.C., P. J. DeMott, S.M. Kreidenweis, and Y. Chen, 2001: A continuous flow diffusion chamber for airborne measurements of ice nuclei. *J. Atmos. Oceanic Technol.*, **18**, 725-741.
- Rosenfeld, D., 1999: TRMM observed first direct evidence of smoke from forest fires inhibiting rainfall. *Geophys. Res. Lett.*, **26**, 3105-3108.
- Rosenfeld, D., 2000: Suppression of rain and snow by urban and industrial air pollution. *Science*, **287**, 1793-1796.
- Rosenfeld, D., and W.L. Woodley, 1989: Effects of cloud seeding in west Texas. *J. Appl Meteor.*, **28**, 1050-1080.
- Rosenfeld, D., and W.L. Woodley, 1993: Effects of cloud seeding in west Texas: Additional results and new insights. *J. Appl. Meteor.*, **32**, 1848-1866.
- Sassen, K., P.J. DeMott, J.M. Prospero, and M.R. Poellet, 2003: Saharan dust storms and indirect aerosol affects on clouds: CRYSTAL-FACE Results. *Geophys. Res. Lett.*, **30**, doi:10.1029/2003GL017371.
- Saleeby, S.M., and W.R. Cotton, 2004: A large-droplet mode and prognostic number concentration of cloud droplets in the Colorado State University Regional Atmospheric Modeling System (RAMS). Part I: Module descriptions and supercell test simulations. *J. Appl. Meteor.*, **43**, 182-195.
- Schaefer, V.J., 1949: The formation of ice crystals in the laboratory and the atmosphere. *Chem. Rev.*, **44**, 291.
- Schaefer, V.J., 1954: The concentrations of ice nuclei in air passing the summit of Mt. Washington. *Bull. Amer. Meteor. Soc.*, **35**, 310-314.
- Simpson, J., G.W. Brier, and R.H. Simpson, 1967: STORMFURY cumulus seeding experiment 1965: Statistical analysis and main results. *J. Atmos. Sci.*, **24**, 508-521.
- Stein, U., and P. Alpert, 1993: Factor separation in numerical simulations. *J. Atm. Sci.*, **50**, 2107-2115.
- VanReken, T. M., T. A. Rissman, G. C. Roberts, V. Varutbangkul, H. H. Jonsson, R. C. Flagan, and J. H. Seinfeld, 2003: Toward aerosol/cloud condensation nuclei (CCN) closure during CRYSTAL-FACE. *J. Geophys. Res.*, **108**, 4633, doi:10.1029/2003JD003582.
- Warner, J. and S. Twomey, 1967: Comparison of measurements of cloud droplets and cloud nuclei. *J. Atmos. Sci.*, **24**, 702-703.